Journal of Organometallic Chemistry 694 (2009) 339–345

Contents lists available at ScienceDirect

Journal of Organometallic Chemistry

journal homepage: www.elsevier.com/locate/jorganchem

Syntheses, characterization and sensitized lanthanide luminescence of heteronuclear Pt–Ln (Ln = Eu, Nd, Yb) complexes with 2,2′-bipyridyl ethynyl ligands

Jun Ni [a], Li-Yi Zhang [a], Zhong-Ning Chen [a,b,*]

[a] State Key Laboratory of Structural Chemistry, Fujian Institute of Research on the Structure of Matter, Chinese Academy of Sciences, No. 155 West Road of Yangqiao, Fuzhou, Fujian 350002, China
[b] State Key Laboratory of Organometallic Chemistry, Shanghai Institute of Organic Chemistry, Chinese Academy of Sciences, Shanghai 200032, China

ARTICLE INFO

Article history:
Received 6 September 2008
Received in revised form 27 October 2008
Accepted 31 October 2008
Available online 6 November 2008

Keywords:
Alkynyl ligand
Energy transfer
Lanthanide
Luminescence
Platinum

ABSTRACT

Reaction of $[Pt(Bu^t_3tpy)Cl]^+$ (Bu^t_3tpy = 4,4′,4″-tri-*tert*-butyl-2,2′:6′,2″-terpyridine) with 5-ethynyl-2,2′-bipyridine (HC≡Cbpy) or 5,5′-bis(trimethylsilylethynyl)-2,2′-bipyridine ($Me_3SiC{\equiv}CbpyC{\equiv}CSiMe_3$) in the presence of cuprous iodide gives $[Pt(^tBu_3tpy)(C{\equiv}Cbpy)]^+$ (**1**) or $[\{Pt(Bu^t_3tpy)\}_2(C{\equiv}CbpyC{\equiv}C)]^{2+}$ (**2**) through Pt-acetylide σ-coordination, respectively. Incorporating **1** or **2** with $Ln(hfac)_3(H_2O)_2$ through 2,2′-bipyridyl chelating the Ln^{III} (Ln = Nd, Eu, and Yb) centers induces formation of a series of $[Pt(Bu^t_3tpy)(C{\equiv}Cbpy)\{Ln(hfac)_3\}]^+$ (PtLn) or $[\{Pt(Bu^t_3tpy)\}_2(C{\equiv}CbpyC{\equiv}C)\{Ln(hfac)_3\}]^{2+}$ (Pt_2Ln) complexes, respectively. The structures of binuclear platinum(II) complex $\mathbf{2}(PF_6)_2$ and heterobinuclear PtNd complex $\mathbf{3}(CF_3COO)$ were determined by single crystal X-ray diffraction. Both **1** and **2** exhibit typical low-energy absorption bands in near UV–Vis region, ascribed to $d\pi(Pt) \rightarrow \pi^*(Bu^t_3tpy)$ MLCT and $\pi(C{\equiv}Cbpy/C{\equiv}CbpyC{\equiv}C) \rightarrow \pi^*(Bu^t_3tpy)$ LLCT transitions. Upon formation of the PtLn or $PtLn_2$ complexes, the low-energy absorption bands are obviously blue-shifted (15–20 nm) compared with those in the Pt^{II} precursor **1** or **2**. With excitation at 350 nm < λ < 550 nm which is the absorption region of MLCT and LLCT transitions, sensitized luminescence that is characteristic of the corresponding lanthanide(III) ions occurs in both PtLn and Pt_2Ln complexes. In contrast, Pt-based luminescence from the MLCT and LLCT states are mostly quenched in these Pt–Ln heteronuclear complexes, revealing that quite effective Pt → Ln energy transfer is operating from the $Pt(Bu^t_3tpy)$(acetylide) chromophore to the lanthanide(III) centers.

1. Introduction

The chemistry of metal alkynyl complexes is of intense current interest in view of the extensive applications of these compounds as molecular wires, luminescent sensors, light emitting materials and nonlinear optical materials [1–8]. Compared with the simple alkynes, functionalized alkynyl ligands are more favorable for fabrication of heteronuclear and/or multicomponent complexes that contain different types of organometallic subunits as chromophores and/or emitters. Of various functionalized alkynes, polypyridyl alkynyl ligands are particularly useful in design of heteronuclear and/or multicomponent complexes with desired electronic and optical properties [9,10]. On the one hand, the favorable π-conjugacy makes them excellent candidates as mediators for intercomponent electron/energy transfer. On the other hand, the bifunctional character favors multicomponent structural fabrication in a stepwise approach, in which the "soft" alkynyl is always bound to d-block organometallic subunit through σ-coordination and the "hard" polypyridyl frequently associated with another transition metal or lanthanide component. This opens a feasible strategy to access d–f heterometallic arrays containing both d-block metal alkynyl chromphores and lanthanide emitters, allowing effective d → f energy transfer to occur from the former to the latter and thus achieving sensitized luminescence from the corresponding lanthanide ions [11–16].

Platinum(II) terpyridyl alkynyl complexes exhibit intense absorption spectral bands in near UV region extended to visible region, arising from both $d\pi$ (Pt) → π^*(tpy) MLCT and π (alkynyl) → π^*(tpy) LLCT transitions [17,18]. Upon excitation of these platinum(II) complexes at near UV region, they emit brightly visible light. By judicious modification of substituents in the terpyridyl and/or alkynyl ligands, the light emitting colors are changeable [17–23]. The intense light absorption character in UV–Vis region makes them act as excellent light-harvesting antennae to photosensitize d-block metal emitting or lanthanide luminescence [16,24–26]. Particularly, as a consequence of Pt → Ln energy

* Corresponding author. Address: State Key Laboratory of Structural Chemistry, Fujian Institute of Research on the Structure of Matter, Chinese Academy of Sciences, No. 155 West Road of Yangqiao, Fuzhou, Fujian 350002, China. Tel.: +86 591 8379 2346.
E-mail address: czn@fjirsm.ac.cn (Z.-N. Chen).

0022-328X/$ - see front matter © 2008 Elsevier B.V. All rights reserved.
doi:10.1016/j.jorganchem.2008.10.051

transfer from platinum(II) terpyridyl alkynyl subunits to lanthanide(II) centers, sensitized lanthanide luminescence would be achieved. By these considerations, a series of PtLn and Pt_2Ln heternuclear complexes were prepared using 5-ethynyl-2,2′-bipyridine (HC≡Cbpy) and 5,5′-diethynyl-2,2′-bipyridine (HC≡CbpyC≡CH) as bridging ligands, respectively. The platinum(II) terpyridyl chromophore is bonded to the 2,2′-bipyridyl alkynyl ligand through Pt-acetylide σ-coordination whereas $Ln(hafc)_3$ subunit is chelated by 2,2′-bipyridyl. These Pt–Ln complexes exhibit luminescence that is characteristic of the corresponding lanthanide(III) ions whereas the emission from platinum(II) terpyridyl alkynyl chromophore is mostly quenched, revealing that quite effective Pt→Ln energy transfer is operating in these bicomponent arrays.

2. Experimental

2.1. Materials and reagents

All operations were carried out under a dry argon atmosphere using vacuum-line systems and Schlenk techniques unless otherwise specified. The solvents were dried, distilled, and degassed prior to use except that those for spectroscopic measurements were of spectroscopic grade. The 5,5′-bis(trimethylsilylethynyl)-2,2′-bipyridine ($Me_3SiC{\equiv}CbpyC{\equiv}CSiMe_3$) [27], 5-ethynyl-2,2′-bipyridine (HC≡Cbpy) [27], 4,4′,4″-tri-*tert*-butyl-2,2′:6′,2″-terpyridine (Bu^t_3tpy) [28], [$Pt(Bu^t_3tpy)Cl$]X (X = PF_6, ClO_4) [29], and $Ln(hfac)_3(H_2O)_2$ [30] were prepared by the procedures described in literatures.

CAUTION: Perchlorate salts are potentially explosive and should be handled with care and in small amounts.

2.2. Preparation of [{$Pt(Bu^t_3tpy)$}(C≡Cbpy)][PF_6) (**1**)

[$Pt(Bu^t_3tpy)Cl$](PF_6) (77.7 mg, 0.10 mmol), HC≡Cbpy (18 mg, 0.1 mmol), CuI (1 mg) and diisopropylamine (2 mL) in 50 mL of dichloromethane were stirred at room temperature for 1 d. After the solvents were removed in vacuo, the residue was dissolved in a small amount of dichloromethane. The product was then purified by chromatography on a silica gel column using dichloromethane–methanol (10:1 v/v) as eluent to give an air-stable yellow solid. Yield: 60% (65 mg). Anal. Calc. for $C_{39}H_{42}F_6N_5PPt \cdot 2CH_2Cl_2$: C, 45.15; H, 4.25; N, 6.42. Found: C, 44.83; H, 4.46; N, 6.55%. ESI-MS (*m*/*z*): 776 [M−PF_6]$^+$. ^{1}H NMR spectrum (300 MHz, DMSO-d_6, ppm): 1.42 (s, 18H, C_4H_9), 1.51 (s, 9H, C_4H_9), 7.44 (s, 1H, bpy), 7.85 (d, 2H, *J* = 5.1 Hz, bpy), 7.94 (d, 2H, *J* = 7.5 Hz, bpy), 8.36 (s, 2H, tpy), 8.69 (d, 4H, *J* = 4.5 Hz, bpy and tpy), 8.78 (s, 2H, tpy), 8.98 (d, 2H, *J* = 6 Hz, tpy). IR (KBr disk, cm^{-1}): 2116 m (C≡C), 838 m (PF_6).

2.3. Preparation of [{$Pt(Bu^t_3tpy)$}$_2$(C≡CbpyC≡C)][ClO_4)$_2$ (**2**)

To a dichloromethane (40 mL) solution of $Me_3SiC{\equiv}CbpyC{\equiv}CSiMe_3$ (34.8 mg, 0.10 mmol) was added a methanol (10 mL) solution of potassium fluoride (17 mg, 0.30 mmol) with stirring for 30 min. [$Pt(Bu^t_3tpy)Cl$](ClO_4) (146 mg, 0.20 mmol), CuI (2 mg) and diisopropylamine (2 mL) were then added successively. After the solution was stirred at room temperature for 12 h, the solvents were removed in vacuo. The crude product was purified by chromatography on a silica gel column using dichloromethane–methanol (v/v = 10:1) as eluent. Yield: 73% (116 mg). Anal. Calc. for $C_{68}H_{76}Cl_2N_8O_8Pt_2$: C, 51.22; H, 4.80; N, 7.03. Found: C, 51.44; H, 4.66; N, 6.98%. ESI-MS (*m*/*z*): 697 [M−2ClO_4]$^{2+}$. ^{1}H NMR (500 MHz, CD_3CN, ppm): 1.46 (s, 36H, tpy), 1.54 (s, 18H, tpy), 7.90 (d, 4H, *J* = 5.7 Hz, tpy), 7.98 (dd, 2H, *J* = 2.5 Hz, *J* = 2.5 Hz, bpy), 8.33 (d, 2H, *J* = 7 Hz, bpy), 8.71 (s, 8H, tpy), 8.80 (s, 2H, bpy), 9.06 (d, 4H, *J* = 5.5 Hz, tpy). IR (KBr disk, cm^{-1}): 2117 m (C≡C), 1100 m (ClO_4).

2.4. Preparation of [$Pt(Bu^t_3tpy)$(C≡Cbpy){Ln(hfac)$_3$}](PF_6) (Ln = Nd **3**, Eu **4**, Yb **5**)

These compounds were prepared by reactions of **1** with 1.2 equiv. of $Ln(hfac)_3(H_2O)_2$ in dichloromethane with stirring for 30 min at room temperature. After filtered, the solutions were concentrated to precipitate the yellow products by addition of *n*-hexane. Layering *n*-hexane onto the concentrated dichloromethane solutions in the absence of light gave the products as yellow crystals in a few days.

3. Yield 72%. Anal. Calc. for $C_{54}H_{45}F_{24}N_5NdO_6PPt$: C, 38.46; H, 2.69; N, 4.15. Found: C, 38.55; H, 2.73; N, 4.18%. IR (KBr disk, cm^{-1}): 2123m (C≡C); 836s (PF_6); 1654s (C=O).
4. Yield 80%. Anal. Calc. for $C_{54}H_{45}EuF_{24}N_5O_6PPt$: C, 38.29; H, 2.68; N, 4.13. Found: C, 38.42; H, 2.58; N, 4.10%. IR (KBr disk, cm^{-1}): 2125m (C≡C); 833s (PF_6); 1650s (C=O).
5. Yield 75%. Anal. Calc. for $C_{54}H_{45}F_{24}N_5O_6PPtYb \cdot CH_2Cl_2$: C, 36.70; H, 2.63; N, 3.89. Found: C, 36.88; H, 2.68; N, 3.85%. IR (KBr disk, cm^{-1}): 2125m (C≡C); 833s (PF_6); 1650s (C=O).

2.5. Preparation of [{$Pt(Bu^t_3tpy)$}$_2$(C≡CbpyC≡C){Ln(hfac)$_3$}](ClO_4)$_2$ (Ln = Nd **6**, Eu **7**, Yb **8**)

These Pt_2Ln complexes were prepared by the same synthetic procedures as those of the corresponding PtLn complexes except using **2** instead of **1** as the starting material.

3. Yield 85%. Anal. Calc. for $C_{83}H_{79}Cl_2F_{18}N_8NdO_{14}Pt_2 \cdot 2H_2O$: C, 41.61; H, 3.49; N, 4.68. Found: C, 41.68; H, 3.41; N, 4.78%. IR (KBr disk, cm^{-1}): 2119m (C≡C); 1100s (ClO_4); 1652s (C=O).
4. Yield 82%. Anal. Calc. for $C_{83}H_{79}Cl_2EuF_{18}N_8O_{14}Pt_2$: C, 42.11; H, 3.36; N, 4.73. Found: C, 41.95; H, 3.47; N, 4.55%. **IR** (KBr disk, cm^{-1}): 2120m (C≡C); 1098s (ClO_4); 1654s (C=O).
5. Yield 79%. Anal. Calc. for $C_{83}H_{79}Cl_2F_{18}N_8O_{14}Pt_2Yb \cdot CH_2Cl_2$: C, 40.79; H, 3.30; N, 4.53. Found: C, 40.88; H, 3.27; N, 4.48%. IR (KBr disk, cm^{-1}): 2123m (C≡C); 1099s (ClO_4); 1654s (C=O).

2.6. Crystal structure determination

Crystals suitable for X-ray diffraction studies were obtained by layering diethyl ether onto the acetonitrile solution for **2**(PF_6)$_2$ (prepared by metathesis of perchlorate in **2** with sodium hexafluorophosphate) and by layering *n*-heptane onto the dichloromethane solution for **3**(CF_3COO) (prepared by metathesis of hexafluorophosphate in **3** with sodium trifluoroacetate). Single crystals sealed in capillaries with mother liquors were measured on a RIGAKU MERCURY CCD diffractometer by ω scan technique at room temperature with graphite-monochromated Mo Kα radiation (λ = 0.71073 Å). The CRYSTALCLEAR software package was used for data reduction and empirical absorption correction. The structures were solved by direct method. The heavy atoms were located from E-map, and the rest of the non-hydrogen atoms were found in subsequent Fourier maps. Most of the non-hydrogen atoms were refined anisotropically except for some disordered F atoms, whereas the hydrogen atoms were generated geometrically with isotropic thermal parameters. The structures were refined on F^2 by full-matrix least-squares methods using the SHELXTL-97 program package [31]. For some disordered –CF_3 groups, restrained refinements were carried out by fixing the C–F distances at 1.31 Å with

Table 1
Crystallographic data for **2**$(PF_6)_2$ and **3**(CF_3COO).

Compound	**2**$(PF_6)_2$	**3**(CF_3COO)
Empirical formula	$C_{68}H_{76}F_{12}N_8P_2Pt_2$	$C_{56}H_{45}F_{21}N_5NdO_8Pt$
Temperature (K)	293(2)	293(2)
Space group	$P2_1/c$	$C2/c$
a (Å)	10.656(4)	20.397(7)
b (Å)	16.212(6)	23.576(8)
c (Å)	19.917(8)	28.287(10)
β (°)	100.29(1)	110.379(5)
V (Å^3)	3385(2)	12751(8)
Z	2	8
ρ_{calcd}, (g/cm^{-3})	1.653	1.723
μ (mm^{-1})	4.255	3.113
Radiation (λ, Å)	0.71073	0.71073
$R_1(F_o)$[a]	0.0535	0.0787
$wR_2(F_o)$[b]	0.1327	0.2144
Goodness-of-fit (GOF)	1.164	1.053

[a] $R_1 = \Sigma|F_o - F_c|/\Sigma F_o$.
[b] $wR_2 = \sum[w(F_o^2 - F_c^2)^2]/\sum[w(F_o^2)]^{1/2}$.

the occupancy factors of a pair of the corresponding F atoms being 0.50, respectively. The crystallographic data of **2**(PF_6) and **3**(CF_3COO) are summarized in Table 1.

2.7. Physical measurements

Elemental analyses (C, H, N) were carried out on a Perkin–Elmer model 240C elemental analyzer. Infrared (IR) spectra were recorded on a Magna750 FT-IR spectrophotometer with KBr pellet. Electrospray ion mass spectra (ESI-MS) were performed on a Finnigan LCQ mass spectrometer using dichloromethane–methanol mixture as mobile phases. ^{1}H NMR spectra were performed on a Bruker-300 (for **1**) or Bruker-500 (for **2**) in DMSO-d_6 (for **1**) or CD_3CN (for **2**) solution with $SiMe_4$ as the internal reference. UV–Vis absorption spectra in dichloromethane solutions were measured on a Perkin–Elmer Lambda 25 UV–Vis spectrometer. Emission and excitation spectra in the UV–Vis region were recorded on a Perkin–Elmer LS 55 luminescence spectrometer with a red-sensitive photomultiplier type R928. Near-infrared (NIR) emission spectra were measured on an Edinburgh FLS920 fluorescence spectrometer equipped with a Hamamatsu R5509-72 supercooled photomultiplier tube at 193 K and a TM300 emission monochromator with NIR grating blazed at 1000 nm. The NIR emission spectra were corrected via a calibration curve supplied with the instrument. The emission lifetimes above 10 μs were measured on an Edinburgh Xe900 450 W pulse xenon lamp as the excitation light source. The emission lifetimes below 10 μs were determined on an Edinburgh Analytical Instrument (F900 fluorescence spectrometer) using LED laser at 397 nm excitation and the resulting emission was detected by a thermoelectrically-cooled Hamamatsu R3809 photomultiplier tube. The instrument response function at the excitation wavelength was deconvolved from the luminescence decay. The emission quantum yields (Φ) of **1**, **2**, **4**, and **7** in degassed dichloromethane solutions at room temperature were calculated by $\Phi_s = \Phi_r(B_r/B_s)(n_s/n_r)^2(D_s/D_r)$ using $[Ru(bpy)_3](PF_6)_2$ in acetonitrile as the standard ($\Phi_{em} = 0.062$) [32,33], where the subscripts r and s denote reference standard and the sample solution, respectively; and n, D and Φ are the refractive index of the solvents, the integrated intensity and the luminescence quantum yield, respectively. The quantity B is calculated by $B = 1 - 10^{-AL}$, where A is the absorbance at the excitation wavelength and L is the optical path length. All the solutions used for determination of emission lifetimes and quantum yields were prepared under vacuum in a 10 cm^3 round bottom flask equipped with a side arm 1 cm fluorescence cuvette and sealed from the atmosphere by a quick-release teflon stopper. Solutions used for luminescence determination were prepared after rigorous removal of oxygen by three successive freeze-pump-thaw cycles.

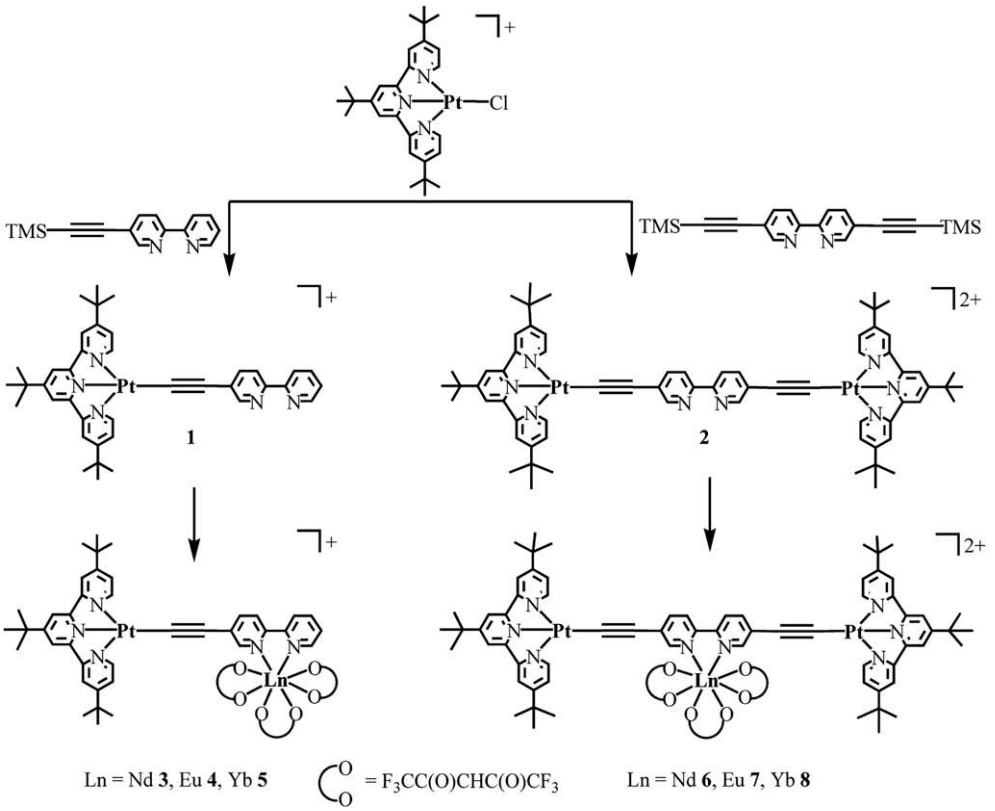

Scheme 1. Synthetic routes to **1**–**9**.

3. Results and discussion

3.1. Syntheses and characterization

As shown in Scheme 1, platinum(II) precursor complexes **1** and **2** were prepared by reactions of $[Pt(Bu^t_3tpy)Cl]^+$ with HC≡Cbpy or Me_3SiC≡CbpyC≡$CSiMe_3$ in dichloromethane solutions in the presence of diisopropylamine, catalyzed by copper(I) iodide, respectively. They were readily purified through chromatography on silica gel columns using dichloromethane–methanol (v/v = 10:1) as eluent. Complexation of **1** or **2** with $Ln(hafc)_3$ units through 2,2′-bipyridyl chelation induced isolation of the corresponding Pt–Ln heterometallic complexes as yellow crystals by layering *n*-hexane onto the concentrated dichloromethane solutions in a few days.

These complexes were characterized by element analyses, ESI-MS spectrometry, IR, ^1H NMR and/or UV–Vis spectroscopy. The structures of **2**(PF_6) and **3**(CF_3COO) were determined by single crystal X-ray diffraction. The IR spectra of **1**–**8** exhibit typical ν(C≡C) bands in the range 2110–2125 cm^{-1}. For Pt–Ln complexes **3**–**8**, the *ν(C═O)* frequency of hfac occurs at ca. 1650 cm^{-1}, confirming the incorporation of $Ln(hfac)_3$ units with **1** or **2** through 2,2′-bipyridyl chelation.

Selected bond lengths and angles of **2**(PF_6) and **3**(CF_3COO) are presented in Table 2. ORTEP drawings of **2**(PF_6) and **3**(CF_3COO) are depicted in Figs. 1 and 2, respectively. The platinum(II) center in **2**(PF_6) adopts a distorted square-planar geometry composed of three N donors from Bu^t_3tpy and one C donor from σ-coordinated acetylide. The sum of the *cis*-angles around the platinum(II) center is ca. 360° and the mean deviation of the $PtCN_3$ atoms from the least-squares plane is 0.008 Å, revealing an excellent coplanarity. The Pt–C≡C–C array is quasi-linear with Pt–C28–C29 = 179.0(1)° and C28–C29–C30 = 176.7(1)°. The Pt–N (1.952(8)–2.036(9) Å) and Pt–C (1.975(10) Å) distances are comparable to those in other platinum(II) terpyridyl acetylide analogues [18,24,25,34]. The 2,2′-bipyridyl rings in the C≡CbpyC≡C form a dihedral angle of 12.9° with the Pt^{II} coordination plane defined by CN_3 donors. The intramolecular Pt···Pt separation through the bridging C≡CbpyC≡C is 16.26 Å. The shortest intermolecular Pt···Pt distance is 4.88 Å, excluding the possibility to form intermolecular Pt–Pt contact.

Heterobinuclear complex **3**(CF_3COO) originates from incorporating $[Pt(Bu^t_3tpy)(C≡Cbpy)](CF_3COO)$ with $Nd(hfac)_3$ unit by chelating Nd^{III} center through 2,2′-bipyridyl. The square-planar platinum(II) center is bonded by CN_3 donors with *cis*-angles in the range 79.5(4)–100.1(5)° and the sum of *cis*-angles being ca. 360°. These bonding parameters together with *trans*-angles around Pt1 center (N2–Pt1–N3 = 160.4(4)° and N2–Pt1–C28 = 178.4(4)°) are all comparable to the corresponding values in platinum(II) precursor complex **2**(PF_6)$_2$. Upon formation of the PtNd array **3**(CF_3COO), the dihedral angle (7.0°) between the least-square plane of terpyridyl and that of C≡Cbpy is smaller than that in **2**(PF_6)$_2$ (12.9°). The Nd^{III} center is nine-coordinated to give a distorted capped square antiprism composed of N_2O_7 donors with the trifluoroacetate O donor at the capping site. Intramolecular Pt···Nd separation through the bridging C≡Cbpy is 8.89 Å. The shortest intermolecular Pt···Pt distance is 5.62 Å, implying the absence of Pt–Pt contact.

Table 2
Selected bond distances (Å) and angles (°) for **2**(PF_6)$_2$ and **3**(CF_3COO).

***2**(PF$_6$)$_2$*			
Pt1–N1	2.036(9)	Pt1–N1	2.031(9)
Pt1–N1	1.951(8)	Pt1–C28	1.977(9)
C28–C29	1.194(13)		
N2–Pt1–C28	178.9(4)	C28–Pt1–N3	100.8(4)
N2–Pt1–N1	79.5(3)	C28–Pt1–N1	99.5(4)
N3–Pt1–N1	159.7(3)	N2–Pt1–N3	80.2(3)
C29–C28–Pt	170.08(9)		
***3**(CF$_3$COO)*			
Pt1–N2	1.968(9)	Pt1–C28	1.996(13)
Pt1–N1	1.998(11)	Pt1–N3	2.015(12)
Nd1–O1	2.476(8)	Nd1–O2	2.395(7)
Nd1–O3	2.496(10)	Nd1–O4	2.457(8)
Nd1–O5	2.507(9)	Nd1–O6	2.444(10)
Nd1–O7	2.359(8)	Nd1–N4	2.668(8)
Nd1–N5	2.708(7)	C28–C29	1.212(16)
N2–Pt1–C28	178.4(4)	N2–Pt1–N1	80.9(4)
C28–Pt1–N1	99.5(5)	N2–Pt1–N3	79.5(4)
C28–Pt1–N3	100.1(5)	N1–Pt1–N3	160.4(4)
C29–C28–Pt1	171.8(13)	O7–Nd1–O2	79.9(3)
O7–Nd1–O6	146.3(3)	O2–Nd1–O6	131.3(3)
O7–Nd1–O4	100.4(3)	O2–Nd1–O4	136.6(3)
O6–Nd1–O4	67.0(4)	O7–Nd1–O1	136.2(3)
O2–Nd1–O1	73.6(3)	O6–Nd1–O1	73.7(3)
O4–Nd1–O1	77.5(3)	O7–Nd1–O3	74.0(3)
O2–Nd1–O3	71.8(4)	O6–Nd1–O3	122.8(4)
O4–Nd1–O3	66.9(5)	O1–Nd1–O3	64.9(3)
O7–Nd1–O5	130.2(3)	O2–Nd1–O5	69.4(3)
O6–Nd1–O5	66.3(4)	O4–Nd1–O5	128.9(4)
O1–Nd1–O5	70.8(3)	O3–Nd1–O5	127.2(3)
O7––Nd1–N4	72.3(3)	O2–Nd1–N4	83.7(3)
O6–Nd1–N4	96.1(3)	O4–Nd1–N4	138.2(3)
O1–Nd1–N4	136.4(3)	O3–Nd1–N4	141.1(4)
O5–Nd1–N4	66.4(3)	O7–Nd1–N5	74.7(3)
O2–Nd1–N5	141.1(3)	O6–Nd1–N5	72.1(3)
O4–Nd1–N5	77.5(3)	O1–Nd1–N5	143.4(3)
O3–Nd1–N5	126.4(3)	O5–Nd1–N5	106.2(3)
N4–Nd1–N5	60.8(2)		

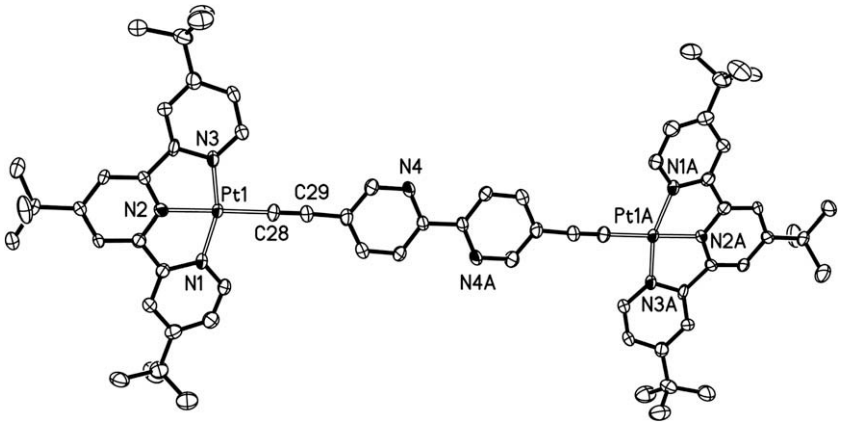

Fig. 1. ORTEP drawing of **2**(PF_6)$_2$ with atom-labeling scheme showing 30% thermal ellipsoids. The hexafluorophosphates are omitted for clarity.

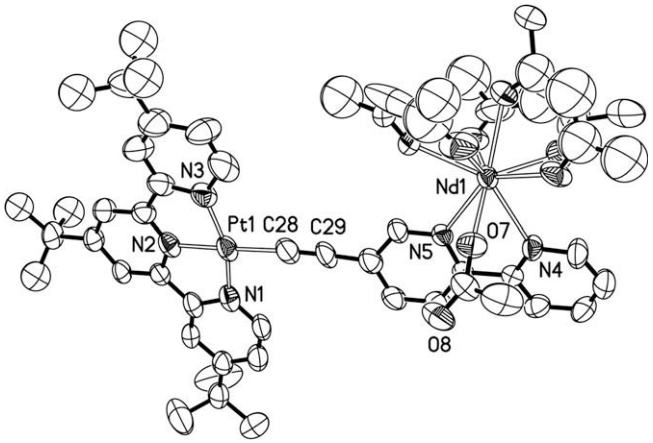

Fig. 2. ORTEP drawing of **3**(CF_3COO) with atom-labeling scheme showing 30% thermal ellipsoids. The F atoms in $-CF_3$ are omitted for clarity.

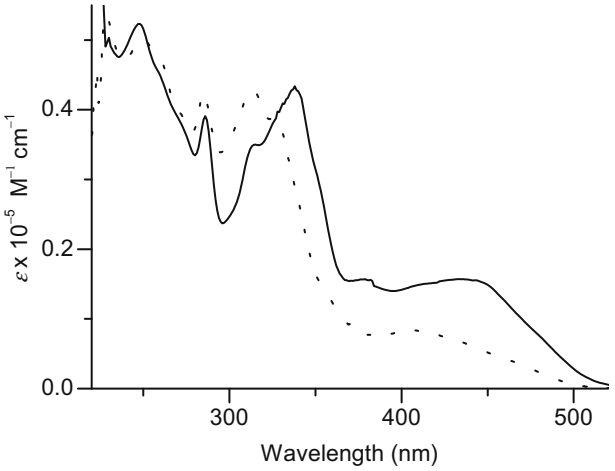

Fig. 3. UV–Vis absorption spectra of **1** (dots) and **2** (solid line) in dichloromethane solutions at room temperature.

3.2. UV–Vis absorption features

The UV–Vis absorption spectral data of **1**–**8** are listed in Table 3. The UV–Vis spectra of **1** and **2** exhibit high-energy absorption bands at 220–290 nm, medium-energy bands at 310–350 nm, and low-energy bands at ca. 412 nm for **1** and 435 nm for **2** tailing to ca. 520 nm. With reference to the absorption features of other platinum(II) terpyridyl alkynyl complexes [18–23], the intense high-energy absorption bands with extinction coefficients (ε) on the order of $10^4\ M^{-1}\ cm^{-1}$ are assigned as intraligand (IL) transitions of the terpyridyl and 2,2′-bipyridyl ligands. The medium-energy absorptions are probably from $\pi \rightarrow \pi^*$(C≡C) transition of the alkynyl ligands. The low-energy absorption bands in UV to visible region arise most likely from d(Pt) → $\pi^*(Bu^t_3tpy)$ MLCT transition, mixed probably with some character from π(C≡Cbpy/C≡CbpyC≡C) → $\pi^*(Bu^t_3tpy)$ LLCT states [19,20,24,25,34,35]. As shown in Fig. 3, both the medium-energy absorption from $\pi \rightarrow \pi^*$(C≡C) transition and the low-energy absorption from MLCT/LLCT states are obviously red-shifted (10–25 nm) and the corresponding absorption intensity is significantly enhanced in **2** compared with those in **1**. This can be ascribed to the more extended π-system in 5,5′-diethynyl-2,2′-bipyridine bridged dinuclear platinum(II) complex **2** than that in mononuclear platinum(II) complex **1** containing 5-ethynyl-2,2′-bipyridine, which induces decrease of the HOMO–LUMO energy gaps for the corresponding electronic transitions in **2**.

Upon formation of the Pt–Ln heteronuclear complexes by incorporating **1** or **2** with $Ln(hafc)_3$ units through 2,2′-bipyridyl chelation, the absorptions from both $\pi \rightarrow \pi^*$(C≡C) transition and MLCT/LLCT states show distinctly blue-shift (15–30 nm) to the higher energy region (Figs. S1 and S2, Supplementary material) relative to those in **1** or **2**. As depicted in Fig. S3 (Supplementary material) or Fig. 4, titration of **1** or **2** by addition of $Yb(hfac)_3(H_2O)_2$ in dichloromethane induced progressive shifts to higher energy region for the absorptions from MLCT/LLCT transitions. This is easily understandable because introducing electron-accepting $Ln(hafc)_3$ units to **1** or **2** would lower the energy level of dπ (Pt) orbitals, thus increasing the energy gap between HOMO (d(Pt)) and LUMO ($\pi^*(Bu^t_3tpy)$) in the MLCT/LLCT states. By comparison of the absorption features between heterobinuclear PtLn and heterotrinuclear Pt_2Ln complexes (Fig. S4, Supplementary material), it is found that both $\pi \rightarrow \pi^*$(C≡C) and MLCT/LLCT absorption bands in the latter are distinctly red-shifted compared with those in the corresponding former. This is due most likely to the more extended π-systems in the $PtLn_2$ complexes, causing reduced HOMO–LUMO energy gaps for the corresponding $\pi \rightarrow \pi^*$(C≡C) and MLCT/LLCT transitions [25,36–39].

Table 3
UV–Vis absorption data of **1**–**8**.

Compound	λ/nm (ε/$M^{-1}\ cm^{-1}$)
1	229(53100), 250(50300), 285(42350), 313(42860), 326(38800), 412(5990), 462(4970)
2	248(48490), 286(35680), 339(42870), 379(13480), 409(12950), 435(15700), 482(7080)
3	228(48710), 250(43430), 303(51050), 422(8980), 452 (5630)
4	229 (38480), 250 (42320), 300 (50810), 422 (8940), 452 (5440)
5	231(31940), 251(39630), 292(54060), 420(8870), 451 (5070)
6	247(54960), 289(54270), 301(60700), 337(37080), 374(27160), 441(19780), 470(9950)
7	246(54200), 289(53050), 311(55780), 337(33900), 374(25720), 442(20400), 471(9860)
8	246(52840), 289(64760), 304(71000), 337(34870), 374(25450), 446(17950) 469(9960)

3.3. Luminescence properties

Luminescence data including emission wavelengths, quantum yields and lifetimes of **1**–**8** are summarized in Table 4. With excitation at λ_{ex} > 300 nm, both **1** and **2** emit brightly yellow to orange

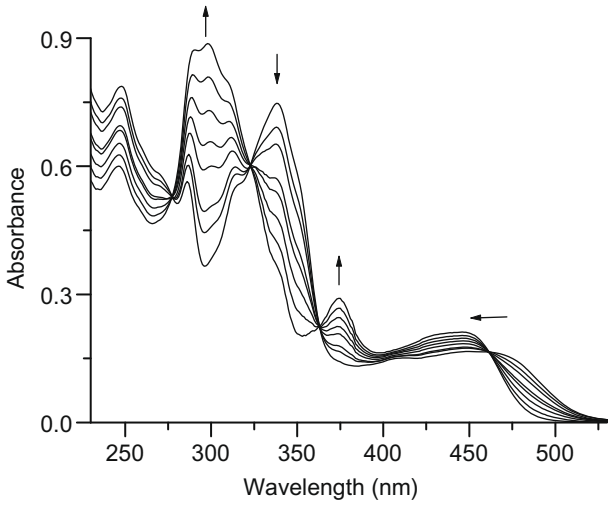

Fig. 4. Changes in the UV–Vis absorption spectra by titration of **2** with $Yb(hfac)_3(H_2O)_2$ in dichloromethane solutions.

emission in both solid states and fluid dichloromethane solutions (Figs. S5 and S6, Supplementary material). The lifetimes are in the microsecond ranges in both solid states and degassed dichloromethane solutions at room temperature. These behaviors are characteristic of platinum(II) tripyridyl alkynyl complexes with the emissive origins from d(Pt) → π*(Bu$^t_3$tpy) ^{3}[MLCT] excited triplet state, mixed probably with some character from π(C≡Cbpy/C≡CbpyC≡C) → π*(Bu$^t_3$tpy) ^{3}[LLCT] transition [19,20,24,25,34,35]. The emission of **2** occurs at a lower energy compared with that of **1** in both solid state (Fig. S5, Supplementary material) and fluid dichloromethane solution (Fig. S6, Supplementary material). As the more extended π-conjugated system in **2** would raise the energy level of d(Pt) orbital (HOMO) through pπ–dπ overlap, the energy gaps between HOMO [d(Pt)/π(C≡CbpyC≡C)] and LUMO [π*(Bu$^t_3$tpy)] would be reduced [25], thus inducing a red shift of the MLCT/LLCT absorption in diplatinum(II) species **2** compared with that in Pt^{II} mononuclear complex **1**.

Upon excitation at 350 nm < λ_{ex} < 550 nm which is the absorption region of d(Pt) → π*(Bu$^t_3$tpy) MLCT and π(C≡Cbpy/C≡CbpyC≡C) → π*(Bu$^t_3$tpy) LLCT transitions, Pt–Ln heteronuclear complexes **3**–**8** exhibit luminescence that is characteristic of the corresponding lanthanide(III) ions (Figs. S7–S10, Supplementary material). The lifetimes of lanthanide-based luminescence are in the microsecond range in both solid states and dichloromethane solutions except that Nd-based emissions are too weak to be measured (Table 4). As indicated in Fig. 5 and Figs. S7–S10 (Supplementary material), three emission bands are observed for Pt–Nd complexes at ca. 870, 1060, and 1335 nm due to $^4F_{3/2} \rightarrow {}^4I_{9/2}$, $^4I_{11/2}$, $^4I_{13/2}$ transitions, four for Pt–Eu complexes at 595, 613, 650, and 695 nm due to $^5D_0 \rightarrow {}^7F_1$, $^7F_2$, $^7F_3$ and $^7F_4$, and one for Pt–Yb complexes at ca. 980 nm due to $^2F_{5/2} \rightarrow {}^2F_{7/2}$ transition. As the model complex Eu(hfac)$_3$(bpyC≡C) lacks of intensity at λ > 350 nm in the excitation spectrum (Fig. S11, Supplementary material), the sensitized lanthanide emission of Pt–Ln heteronuclear complexes should originate from energy transfer from the platinum(II) terpyridyl alkynyl antenna chromophore [10–16].

In contrast with occurrence of sensitized lanthanide luminescence, the Pt^{II}-based broad emission in the visible region, however, is mostly quenched in these Pt–Ln complexes except for Pt$_2$Eu complex **7** due to the severely spectral overlapping between Pt- and Eu-based emissions (Figs. S9 and S10, Supplementary material) which is unfavorable to Pt → Eu energy transfer because of the unmatched energy levels. As shown in Fig. 6, upon formation of the PtYb array by titration of **1** with Yb(hfac)$_3$(H$_2$O)$_2$ in dichloromethane solution, while the Yb-centered emission is progressively enhanced, the Pt-based emission from MLCT/LLCT states is remarkably attenuated so as to be completely quenched when 1 equiv. of

Table 4
Luminescence data of **1–9** at 298 K.

Compound	λ_{em}/nm (τ_{em}/μs) (solid)[a]	λ_{em}/nm (τ_{em}/μs) (CH_2Cl_2)[a]	Φ (%)[b,c]
1	576 (1.5)	570 (2.1)	3.3
2	577 (2.7), 614sh	578 (2.3)	3.6
3	1061 (weak)	1061 (weak)	
4	613 (257)	613 (506)	14.5
5	978 (13.5)	978 (11.5)	0.57
6	1061 (weak)	1061 (weak)	
7	613 (125.3, 41.4)	613 (124.8, 31.6)	6.7
8	978 (14.3)	978 (12.2)	0.61

[a] The excitation wavelength in the lifetime measurement is 397 nm.
[b] The quantum yields of complexes **1**, **2**, **4**, and **7** in degassed dichloromethane are determined relative to that of [Ru(bpy)$_3$](PF$_6$)$_2$ (Φ = 0.062) in degassed acetonitrile [32].
[c] The quantum yields of Yb^{III} complexes in dichloromethane solution are estimated by the equation $\Phi = \tau_{obs}/\tau_0$, in which τ_{obs} is the observed emission lifetime and τ_0 is the radiative or 'natural' lifetime with 2 ms. These values refer to the lanthanide-based emission process only and take no account for the efficiency of intersystem crossing and energy transfer processes.

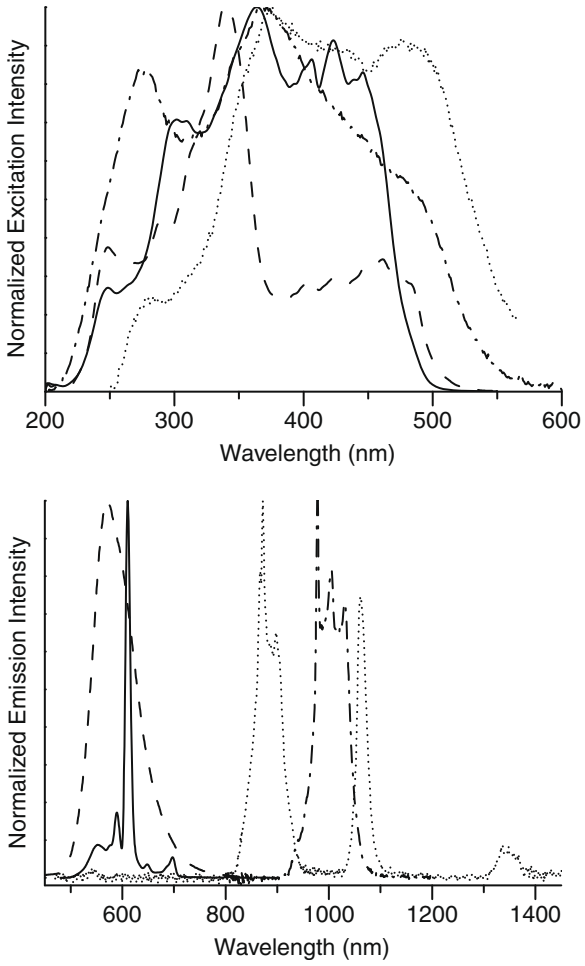

Fig. 5. Excitation (top) and emission (lower) spectra of **2** (dashes), **6** (dots), **7** (solid line) and **8** (dash dots) in fluid dichloromethane solutions.

Yb(hfac)$_3$(H$_2$O)$_2$ is added. The entire quenching of Pt-based luminescence in these Pt–Ln complexes except for **7** in solid state together with the observation of sensitized lanthanide luminescence with excitation at the absorption region of Pt-based chromophore reveals unambiguously that quite effective Pt → Ln energy

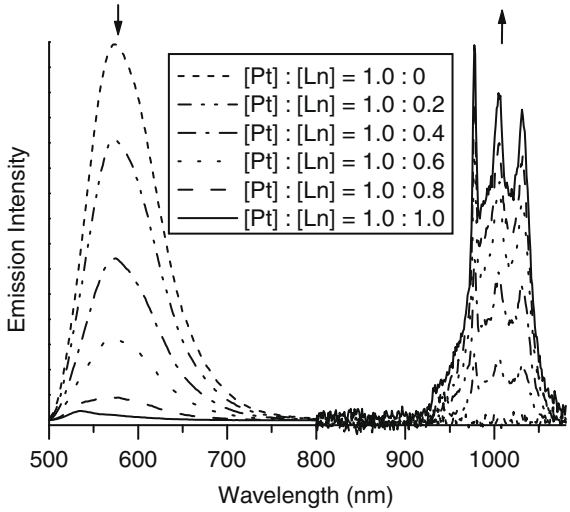

Fig. 6. Titration of **1** with Yb(hfac)$_3$(H$_2$O)$_2$ in dichloromethane, showing both quenching of Pt(Bu$^t_3$tpy)(acetylide) chromophore-based emission and increasing of Yb-centered emission by gradual addition of Yb(hfac)$_3$(H$_2$O)$_2$.

transfer is operating in these Pt–Ln heteronuclear complexes [9–16].

4. Conclusions

Mono- or dinuclear platinum(II) complex of 5-ethynyl-2,2′-bipyridine or 5,5′-diethynyl-2,2′-bipyridine capped with one or two $[Pt(Bu^t_3tpy)_2]^+$ units was synthesized through Pt-acetylide σ-coordination, respectively. They emit brightly yellow to orange room temperature luminescence, arising from $d(Pt) \rightarrow \pi^*(Bu^t_3tpy)$ ^{3}[MLCT] and $\pi(C{\equiv}Cbpy/C{\equiv}CbpyC{\equiv}C) \rightarrow \pi^*(Bu^t_3tpy)$ ^{3}[LLCT] triplet excited states. This makes them serve as favorable energy donors to attain sensitized lanthanide luminescence by energy transfer from the platinum(II) terpyridyl alkynyl chromophores to the lanthanide centers in a series of Pt–Ln heteronuclear complexes resulting from incorporation of mono- or dinuclear platinum(II) precursors with $Ln(hfac)_3$ units. With excitation λ_{ex} at the absorption region of MLCT/LLCT states in platinum(II) terpyridyl alkynyl chromophores, the Pt–Ln heteronuclear complexes emit characteristic lanthanide luminescence with emissive lifetime in microsecond ranges whereas the Pt-based luminescence are mostly quenched because of quite effective $Pt \rightarrow Ln$ energy transfer from Pt-based chromophores to lanthanide(III) centers.

Acknowledgements

This work was financially supported by the NSFC (Grants 20521101, 20625101 and 20773128), the 973 project (Grant 2007CB815304) from MSTC, the NSF of Fujian Province (Grants 2006F3131 and 2008I0027), and the Key Project from CAS (Grant KJCX2-YW-H01).

Appendix A. Supplementary material

Additional UV–Vis absorption and emission spectra, and X-ray crystallographic files in CIF format for the structure determination of **2**$(PF_6)_2$ and **3**(CF_3COO). Supplementary data associated with this article can be found, in the online version, at doi:10.1016/j.jorganchem.2008.10.051.

References

[1] N.J. Long, C.K. Williams, Angew. Chem., Int. Ed. 42 (2003) 2586.
[2] T. Ren, Organometallics. 24 (2005) 4854.
[3] G. Jia, Coord. Chem. Rev. 251 (2007) 2167.
[4] H. Lang, D.S.A. George, G. Rheinwald, Coord. Chem. Rev. 206–207 (2000) 101.
[5] M.I. Bruce, P.J. Low, Adv. Organomet. Chem. 50 (2004) 179.
[6] C.-W. Chan, L.-K. Cheng, C.-M. Che, Coord. Chem. Rev. 132 (1994) 87.
[7] T.C.W. Mak, X.-L. Zhao, Q.-M. Wang, G.-C. Guo, Coord. Chem. Rev. 251 (2007) 2311.
[8] R. Ziessel, M. Hissler, A. El-ghayoury, A. Harriman, Coord. Chem. Rev. 178–180 (1998) 1251.
[9] Z.-N. Chen, Y. Fan, J. Ni, Dalton Trans. (2008) 573.
[10] M.D. Ward, Coord. Chem. Rev. 251 (2007) 1663.
[11] H.-B. Xu, L.-X. Shi, E. Ma, L.-Y. Zhang, Q.-H. Wei, Z.-N. Chen, Chem. Commun. (2006) 1601.
[12] H.-B. Xu, L.-Y. Zhang, Z.-L. Xie, E. Ma, Z.-N. Chen, Chem. Commun. (2007) 2744.
[13] X.-L. Li, F.-R. Dai, L.-Y. Zhang, Y.-M. Zhu, Q. Peng, Z.-N. Chen, Organometallics 26 (2007) 4483.
[14] X.-L. Li, L.-X. Shi, L.-Y. Zhang, H.-M. Wen, Z.-N. Chen, Inorg. Chem. 46 (2007) 10892.
[15] T.K. Ronson, T. Lazarides, H. Adams, S.J.A. Pope, D. Sykes, S. Faulkner, S.J. Coles, M.B. Hursthouse, W. Clegg, R.W. Harrington, M.D. Ward, Chem. Eur. J. 12 (2006) 9299.
[16] R. Ziessel, S. Diring, P. Kadjane, L. Charbonniere, P. Retailleau, C. Philouze, Chem. Asian J. 2 (2007) 975.
[17] K.M.-C. Wong, V.W.-W. Yam, Coord. Chem. Rev. 251 (2007) 2477.
[18] V.W.-W. Yam, R.P.-L. Tang, K.M.-C. Wong, K.-K. Cheung, Organometallics 20 (2001) 4476.
[19] F.N. Castellano, I.E. Pomestchenko, E. Shikhova, F. Hua, M.L. Muro, N. Rajapakse, Coord. Chem. Rev. 250 (2006) 1819.
[20] E. Shikhova, E.O. Danilov, S. Kinayyigit, I.E. Pomestchenko, A.D. Tregubov, F. Camerel, P. Retailleau, R. Ziessel, F.N. Castellano, Inorg. Chem. 46 (2007) 3038.
[21] F. Guo, W. Sun, Y. Liu, K. Schanze, Inorg. Chem. 44 (2005) 4055.
[22] F. Guo, W. Sun, J. Phys. Chem. B 110 (2006) 15029.
[23] Q.-Z. Yang, L.-Z. Wu, Z.-X. Wu, L.-P. Zhang, C.-H. Tung, Inorg. Chem. 41 (2002) 5653.
[24] S.C.-F. Lam, V.W.-W. Yam, K.M.-C. Wong, E.C.-C. Cheng, N. Zhu, Organometallics 24 (2005) 4298.
[25] Y. Fan, L.-Y. Zhang, F.-R. Dai, L.-X. Shi, Z.-N. Chen, Inorg. Chem. 47 (2008) 2811.
[26] C. Monnereau, J. Gomez, E. Blart, F. Odobel, S. Wallin, A. Fallberg, L. Hammarstrom, Inorg. Chem. 44 (2005) 4806.
[27] V. Grosshenny, F.M. Romero, R. Ziessel, J. Org. Chem. 62 (1997) 1491.
[28] T.B. Hadda, H.L. Bozec, Inorg. Chim. Acta 204 (1993) 103.
[29] S.-W. Lai, M.C.W. Chan, K.-K. Cheung, C.-M. Che, Inorg. Chem. 38 (1999) 4262.
[30] Y. Hasegawa, Y. Kimura, K. Murakoshi, Y. Wada, J.-H. Kim, N. Nakashima, T. Yamanaka, S. Yanagida, J. Phys. Chem. 100 (1996) 10201.
[31] G.M. Sheldrick, SHELXL-97, Program for the Refinement of Crystal Structures, University of Göttingen, Göttingen, Germany, 1997.
[32] J.N. Demas, G.A. Crosby, J. Phys. Chem. 75 (1971) 991.
[33] S.C. Chan, M.C.W. Chan, Y. Wang, C.M. Che, K.K. Cheung, N. Zhu, Chem. Eur. J. 7 (2001) 4180.
[34] V.W.-W. Yam, K.M.-C. Wong, N. Zhu, Angew. Chem., Int. Ed. 42 (2003) 1400.
[35] M.L. Muro, F.N. Castellano, Dalton Trans. (2007) 4659.
[36] E.C. Glazer, D. Magde, Y. Tor, J. Am. Chem. Soc. 127 (2005) 4190.
[37] I.E. Pomestchenko, D.E. Polyansky, F.N. Castellano, Inorg. Chem. 44 (2005) 3412.
[38] Y. Yamamoto, M. Shiotsuka, S. Onaka, J. Organomet. Chem. 689 (2004) 2905.
[39] M. Shiotsuka, Y. Yamamoto, S. Okuno, M. Kitou, K. Nozaki, S. Onaka, Chem. Commun. (2002) 590.